



Belle II sensitivity to long-lived dark photons

Torben Ferber^a, Camilo Garcia-Cely^b, Kai Schmidt-Hoberg^{b,*}

^a Institut für Experimentelle Teilchenphysik, Karlsruher Institut für Technologie (KIT), 76131 Karlsruhe, Germany

^b Deutsches Elektronen-Synchrotron DESY, Notkestr. 85, 22607 Hamburg, Germany

ARTICLE INFO

Article history:

Received 20 February 2022

Received in revised form 9 June 2022

Accepted 3 August 2022

Available online 9 August 2022

Editor: A. Ringwald

ABSTRACT

In this letter we point out that the Belle II experiment has a unique sensitivity to visibly decaying long-lived dark photons. Concentrating on the signatures with a single high-energy photon in association with a displaced pair of charged particles, we find that Belle II will be able to probe large regions of parameter space that cannot be covered by any other running or proposed experimental facility. While the signature with charged muons or pions in the final state is expected to be background-free after all selections are applied, the case of final state electrons is more involved and requires an in-depth study. We discuss possible ways to further suppress backgrounds and the corresponding experimental prospects.

© 2022 The Author(s). Published by Elsevier B.V. This is an open access article under the CC BY license (<http://creativecommons.org/licenses/by/4.0/>). Funded by SCOAP³.

1. Introduction

Additional $U(1)$ gauge groups naturally appear in many scenarios beyond the Standard Model and are often part of a so-called ‘hidden sector’ [1–3], which may contain the dark matter particle as well as other weakly coupled states. Even though Standard Model (SM) particles do not necessarily possess direct charges under this $U(1)$ factor, effective couplings between the associated A' gauge boson and SM states can naturally be induced through kinetic mixing with the SM hypercharge field strength [4]. This mixing therefore provides a renormalisable portal through which A' gauge bosons can be produced via the collision of SM particles, and corresponding signatures have been proposed and searched for extensively in recent years covering a very large dark photon mass range [5–25]. In particular, light dark sectors with masses in the MeV to GeV range have triggered a lot of attention [26–35] and the Belle II experiment is known to have excellent sensitivity to many of these scenarios.

Depending on the mass ordering and coupling structure within the dark sector, the A' decays invisibly into dark sector final states [19–21], visibly into SM final states [22–25] or into a combination of both, leading to semi-visible final states [36–40]. In the following we concentrate on the case in which the A' decays visibly. For small mixing angles and small A' masses the effective couplings to the SM are photon-like, so that the A' decays into electrically charged SM particles.

In this letter we point out that the Belle II experiment has a unique sensitivity to a weakly coupled visibly decaying dark photon A' whose decays have a displaced vertex. Specifically, the signature we concentrate on here is a single high-energy photon in association with a displaced pair of charged particles. We find that the regions in parameter space that can be probed by this search correspond to intermediate displacements, larger than those probed by many collider experiments but smaller than those probed via beam dumps. As large parts of this accessible parameter region are not covered by any other running or proposed experiment, Belle II has the potential to significantly extend the overall experimental reach to kinetically mixed dark photons. While non-electron final states will lead to signatures which can be made essentially background-free with a number of simple selections, the case of $A' \rightarrow e^+e^-$ proves much more difficult. We discuss the problematic backgrounds in detail and sketch what needs to be done on the experimental side to reduce them to an acceptable level.

In the next section we briefly introduce our notation. In section 3 we then describe the steps required to evaluate the sensitivity of Belle II to this scenario. Our results are presented in section 4 and we conclude with a short discussion in section 5.

2. A brief recap of dark photons

Many theories beyond the SM exhibit additional $U(1)$ gauge factors. It is well known that the cancellation of gauge anomalies constrains the SM charges under this $U(1)_X$ to only a few possibilities, with the simplest scenario corresponding to vanishing charges of SM fermions. However, even in this case an effective interaction

* Corresponding author.

E-mail addresses: torben.ferber@kit.edu (T. Ferber), camilo.garcia.cely@desy.de (C. Garcia-Cely), kai.schmidt-hoberg@desy.de (K. Schmidt-Hoberg).

between the mass eigenstate dark photon A'_μ and the SM particles can arise from a simple kinetic mixing in the Lagrangian, which is allowed by all symmetries. The Lagrangian including such a kinetic mixing term between the dark $U(1)_X$ and $U(1)_Y$ is given by

$$\mathcal{L} = \mathcal{L}_{\text{SM}} - \frac{1}{4} \hat{X}_{\mu\nu} \hat{X}^{\mu\nu} - \frac{\epsilon}{2c_W} \hat{X}_{\mu\nu} \hat{B}^{\mu\nu}, \quad (2.1)$$

together with additional terms which give rise to a mass for the dark photon - either a Stückelberg mass or a mass arising from a dark Higgs mechanism. In this letter we are agnostic about the mass generation mechanism as our results apply to both cases.

The required gauge-boson diagonalisation has been thoroughly discussed in the literature, see e.g. [41,42]. After the fields have been diagonalised and canonically normalised one obtains the physical Z-boson, the SM photon A_μ , and the dark photon A'_μ . For $m_{A'} \ll m_Z$ as studied in this article, the field A'_μ inherits the coupling structure of the photon to the SM fermions up to a common factor ϵ .

A comprehensive discussion of constraints and future prospects for dark photons in the mass range relevant to us has been presented in [43–46] and we refer to those works for further details. For our plots we adapt the limits from [44]¹ and add limits which were subsequently published from LHCb [23] and NA64 [52], as well as projections from FASER2 [53], LHCb [54], HPS [55], SHiP [56] and DarkQuest [57,58]. In the future also LHeC and FCC-he could become relevant for dark photon searches [59].

3. Dark photons at Belle II

In this letter we concentrate on direct production of a dark photon A' in association with the SM photon γ , with the former subsequently decaying into a pair of charged SM states. This results in a single high-energy photon with a displaced pair of charged particles. We concentrate on the case where the pair of charged particles has a significant displacement to reduce backgrounds from prompt SM processes.

Light dark photons with smaller couplings could also be targeted at a long-lived particle detector near the BelleII interaction point [60]. However, the corresponding region of parameter space is already largely constrained by beam dump experiments and hence of less interest.

3.1. The Belle II experiment

The BelleII experiment at the SuperKEKB accelerator is a next generation B-factory [61] that started physics data taking in 2019. SuperKEKB is a circular asymmetric e^+e^- collider with a nominal collision energy of $\sqrt{s} = 10.58 \text{ GeV}$ and a design instantaneous luminosity of $8 \times 10^{35} \text{ cm}^{-2} \text{ s}^{-1}$. The detector is described in detail in [61].

We study the BelleII sensitivity for a dataset corresponding to an integrated luminosity of 0.5 ab^{-1} , 2 ab^{-1} and 50 ab^{-1} , spanning present and future prospects.

3.2. Event generation

To generate events for the process $e^+e^- \rightarrow \gamma A'$ with subsequent decays of A' we employ MadGraph5_aMC@NLO v2.7.2 [62]. For final states induced by the decays of A' we consider

¹ Specifically we show the limits from BaBar [24], NA48/2 [25], KLOE [47], E141 [48], Orsay [49], U70/NuCal [50,51]. We thank Patrick Foldenauer for providing the corresponding data points.

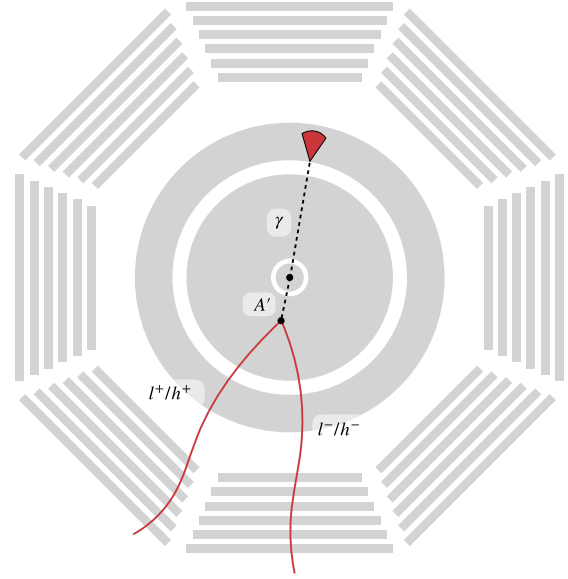


Fig. 1. Schematic view of the BelleII detector (xy -plane) and example displaced signature $e^+e^- \rightarrow \gamma A'$, $A' \rightarrow l^+l^-/h^+h^-$ ($l^\pm = e^\pm, \mu^\pm$ and $h^\pm = \pi^\pm, K^\pm$).

$A' \rightarrow l^+l^-/h^+h^-$ ($l^\pm = e^\pm, \mu^\pm$ and $h^\pm = \pi^\pm, K^\pm$). Given that pions and kaons behave similarly to muons in the BelleII detector, see e.g. the discussion in [39], we do not simulate these particles explicitly. Instead, we rescale the simulated events with final state muons taking into account the relevant branching ratios, which we take from [43]. As in [39] events are generated in the centre-of-mass frame with $\sqrt{s} = 10.58 \text{ GeV}$ and then boosted and rotated to the BelleII laboratory frame.

3.3. Signal selection

Signal events consist of a high-energy photon recoiling against a pair of high-momentum charged particles of opposite charge (see Fig. 1). The two charged particles originate from a common vertex and combine to an invariant mass of the dark photon A' . The two charged particles and the photon together combine to the collision energy of the incoming e^+e^- beams. Experimentally, a vertex fit of the two electrons followed by a kinematic fit of all three particles will improve the invariant mass resolution significantly and allows exploiting the full potential of e^+e^- colliders. For $A' \rightarrow e^+e^-$ we expect that dominant background events for displaced A' decays are $e^+e^- \rightarrow e^+e^-\gamma$ with a misreconstructed prompt decay vertex, and $e^+e^- \rightarrow \gamma\gamma$ followed by a pair conversion $\gamma \rightarrow e^+e^-$; for $A' \rightarrow \mu^+\mu^-/h^+h^-$ the dominant background is $e^+e^- \rightarrow \mu^+\mu^-\gamma$ and $e^+e^- \rightarrow \pi^+\pi^-\gamma$ with a misreconstructed prompt decay vertex, as well as the production and decay of K_S^0 mesons.

As in [39] we select events based on the radial vertex position R of the A' decay products (*region selection*), their trigger signatures (*trigger selection*), and the final state kinematics (*kinematic selection*). The *region selections* are used to select the following vertex regions:

- Decays with $R = \sqrt{x^2 + y^2} < 0.2 \text{ cm}$ are very close to the nominal interaction point and will be subject to large SM backgrounds from $e^+e^- \rightarrow e^+e^-\gamma$ and $e^+e^- \rightarrow \mu^+\mu^-\gamma$ from vertex resolution tails and the geometrical spread of the interaction region. We assume that this region is not suitable for a displaced vertex search. However, this region is generally included in the complementary prompt searches at e^+e^- colliders [24,63].

Table 1
Overview of the various trigger conditions. Table adapted from [65].

Name	Condition	Note
2 GeV energy	At least one calorimeter cluster with $E_{\text{CMS}} > 2 \text{ GeV}$ and $22^\circ < \theta_{\text{lab}} < 139.3^\circ$	Not efficient for muons and hadrons
Two tracks	Two tracks with $38^\circ < \theta_{\text{lab}} < 127^\circ$ and a transverse momentum $p_T > 300 \text{ MeV}$ each, as well as an azimuthal opening angle at the interaction point in the lab system $\Delta\varphi > 90^\circ$	Not efficient beyond a radius of $R_{\text{max}} = 17 \text{ cm}$
1 GeV E sum	The sum of all clusters with $E_{\text{lab}} > 100 \text{ MeV}$ and $27^\circ < \theta_{\text{lab}} < 128^\circ$ is larger than 1 GeV	Muons and hadrons are assumed to contribute at most 200 MeV
Displaced vertex	At least one displaced vertex in the event with $0.9 \text{ cm} < R < 60 \text{ cm}$, formed from two tracks with $p_T > 100 \text{ MeV}$ and $38^\circ < \theta_{\text{lab}} < 127^\circ$ each	Not yet implemented

- The region $0.2 \text{ cm} < R < 0.9 \text{ cm}$ is within the vacuum of the SuperKEKB beam pipe, but sufficiently separated from the interaction point to expect negligible backgrounds from prompt SM backgrounds [64]. While we do not expect any true conversion backgrounds $\gamma \rightarrow e^+e^-$ from $e^+e^- \rightarrow \gamma\gamma$ events, experience from past experiments has shown that a small fraction of conversion events that happen at larger radii will be misreconstructed with a vertex close to the nominal interaction point. Such misreconstructed tracks are often tracks that do not have hits in the inner vertex detector layers, but are extrapolated to a common vertex close to the interaction point by the tracking algorithms. We expect that requiring hits in all detector layers of the Belle II detector downstream of the reconstructed vertex can be used to reduce these backgrounds for $A' \rightarrow e^+e^-$ to small and maybe even negligible levels at the expense of some signal efficiency. Since the number of conversion events is very large, even small misreconstruction rates can lead to sizeable backgrounds. However, these subtle reconstruction effects must be evaluated using full detector simulations for both signal efficiency and background rejection.
- The region $0.9 \text{ cm} < R < 17 \text{ cm}$ includes the beam pipe, the vertex detectors, support structures, and the inner wall of the CDC. This will induce potentially large backgrounds from $\gamma \rightarrow e^+e^-$ from $e^+e^- \rightarrow \gamma\gamma$ events. We expect that these backgrounds are prohibitively large for $A' \rightarrow e^+e^-$, but negligible for $A' \rightarrow \mu^+\mu^-/h^+h^-$. We therefore only consider μ, π , and K in this region.
- $17 \text{ cm} < R < 60 \text{ cm}$ covers the region inside the CDC with sufficiently high tracking efficiency and only small amounts of passive material. We assume that the backgrounds for $A' \rightarrow e^+e^-$ are small, and that the backgrounds for $A' \rightarrow \mu^+\mu^-/h^+h^-$ are negligible.
- For $60 \text{ cm} < R < 150 \text{ cm}$ there will be enough activity in the outer parts of the detector to veto such final states in searches for invisible final states, but not enough information to reconstruct displaced vertices. We do not include this region in our study.

In addition, an event must pass at least one of the *trigger selections* displayed in Table 1 that are the same as in [40,65].² In this work we further assume that photons behave like electrons in the calorimeter-based triggers. We note that for all A' masses accessible in a displaced vertex search at Belle II, the calorimeter cluster triggers are very efficient in triggering on the multi-GeV photon recoiling against the A' .

² In practice we find that for the relevant range in parameter space it would be sufficient to rely on the 2 GeV energy trigger due to the high energy photon present in every signal event.

Table 2
Kinematic selections used in our analysis.

Cut on	Value
Decay vertex	(i) $-55 \text{ cm} \leq z \leq 140 \text{ cm}$ (ii) $17^\circ \leq \theta_{\text{lab}} \leq 150^\circ$
Electrons	(i) both $p(e^+)$ and $p(e^-) > 0.1 \text{ GeV}$ (ii) opening angle of pair $> 0.025 \text{ rad}$ (iii) invariant mass of pair $m_{ee} > 0.03 \text{ GeV}$
μ, π, K	(i) both $p_T(\mu^+)$ and $p_T(\mu^-) > 0.05 \text{ GeV}$ (ii) $m_{ll} < 0.480 \text{ GeV}$ or $m_{ll} > 0.520 \text{ GeV}$
Photons	(i) $E_{\text{lab}} \geq 0.5 \text{ GeV}$ (ii) $17^\circ \leq \theta_{\text{lab}} \leq 150^\circ$

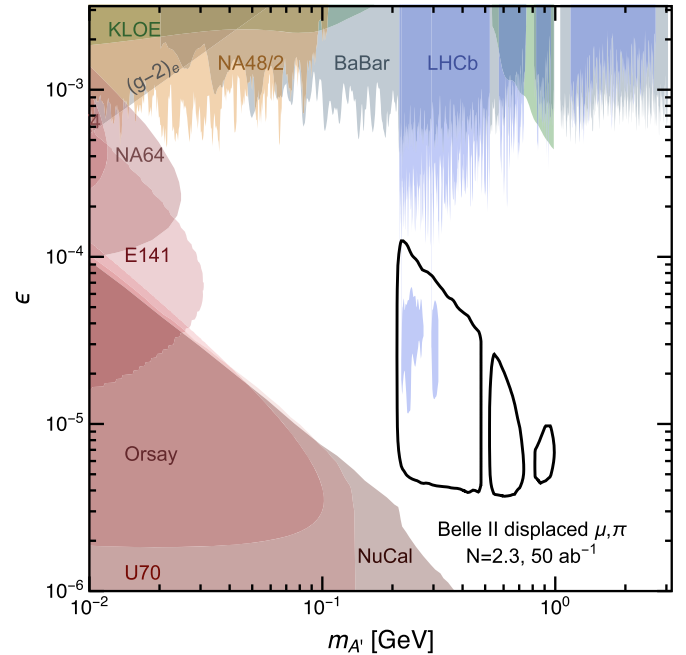


Fig. 2. Expected sensitivity assuming 2.3 events of the search for displaced non-electron final states at Belle II in the $\epsilon - m_{A'}$ parameter plane for an integrated luminosity of 50 ab^{-1} . Existing limits are taken from [44].

Finally the events need to fulfil the *kinematic selection* from Table 2. The requirements on the decay vertex ensure a decay within the tracking detectors of Belle II. For electron final states, we assume that a minimal invariant mass selection of $m_{e^+e^-} \gtrsim 0.03 \text{ GeV}$ and a minimal opening angle of 0.025 rad will be required to reject the majority of conversion background events; for the non-electron final states, we assume that particle identification alone

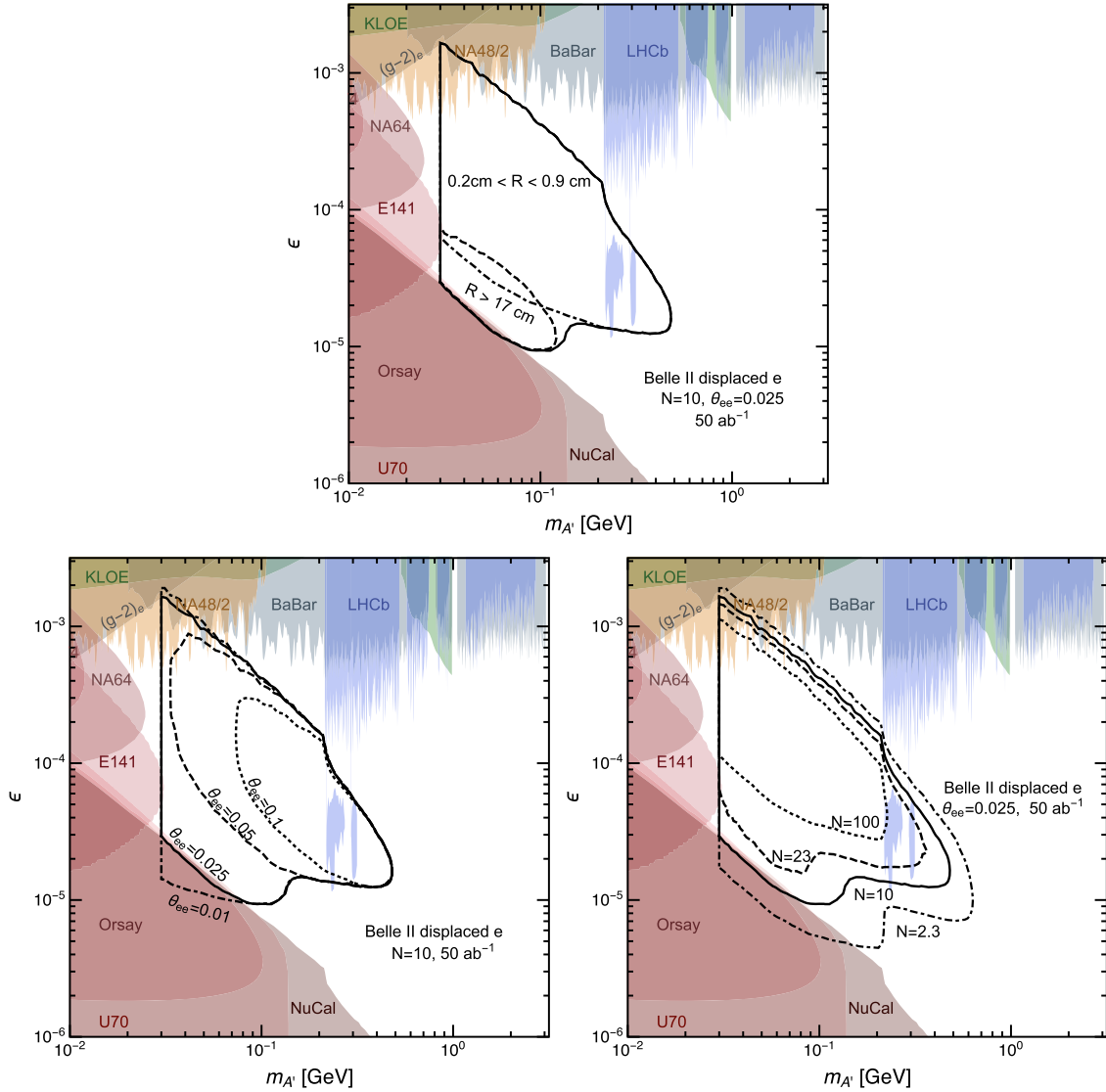


Fig. 3. Expected sensitivity of the search for displaced electron final states at BelleII in the $\epsilon - m_{A'}$ parameter plane for an integrated luminosity of 50 ab^{-1} . In the top panel we show the individual sensitivities corresponding to the regions in which $0.2 \text{ cm} < R < 0.9 \text{ cm}$ (dash-dotted), $17 \text{ cm} < R < 60 \text{ cm}$ (dashed) and the sensitivity for both regions combined (solid) for 10 events and an angular cut $\theta_{ee} = 0.025$. In the bottom panel we show the sensitivity for 10 events and different angular cuts θ_{ee} (left) and a varying number of events for $\theta_{ee} = 0.025$ (right). Existing limits are taken from [44].

is sufficient to reject conversions to a negligible level, but that a mass region around the K_S^0 mass is needed to be cut to reject backgrounds from displaced K_S^0 decays into two pions.

While these selections are motivated by the performance shown in [63], we note that a full study of all possible backgrounds is beyond the scope of this work. In particular, the background for electron final states requires careful studies of reconstruction performance of the BelleII experiment. In a real analysis, energy resolution effects will slightly reduce the signal efficiency. We ignore this effect. We also assume that potentially increasing beam background has a negligible effect on both high momentum track resolution and high-energy photon resolution [63].

4. Results

In this section we split our results into (i) non-electron final states and (ii) final states with electrons. For the sensitivity predictions of non-electron final states we assume zero background after selections. For the case of electrons we discussed sources of background which will not be fully eliminated by the requirements

above and show a number of different sensitivities for different assumptions.

4.1. Sensitivity for non-electron final states

Our main result for the non-electron case is presented in Fig. 2, where we show the expected sensitivity of BelleII to a signature with a single high-energy photon in association with displaced non-electron final states in the $\epsilon - m_{A'}$ parameter plane for an integrated luminosity of 50 ab^{-1} (black solid line) and zero backgrounds. We observe that this search is expected to cover a dark photon mass range $2m_\mu \lesssim m_{A'} \lesssim 1 \text{ GeV}$.³ We find that both regions $0.2 \text{ cm} < R < 0.9 \text{ cm}$ and $0.9 \text{ cm} < R < 17 \text{ cm}$ contribute similarly to the sensitivity, while larger displacements do not add additional sensitivity. In total we expect at most around 50 events for

³ While we include charged kaon final states in our analysis, it is evident from this mass range that they do not contribute significantly to the sensitivity, which is dominated by muon and pion final states.

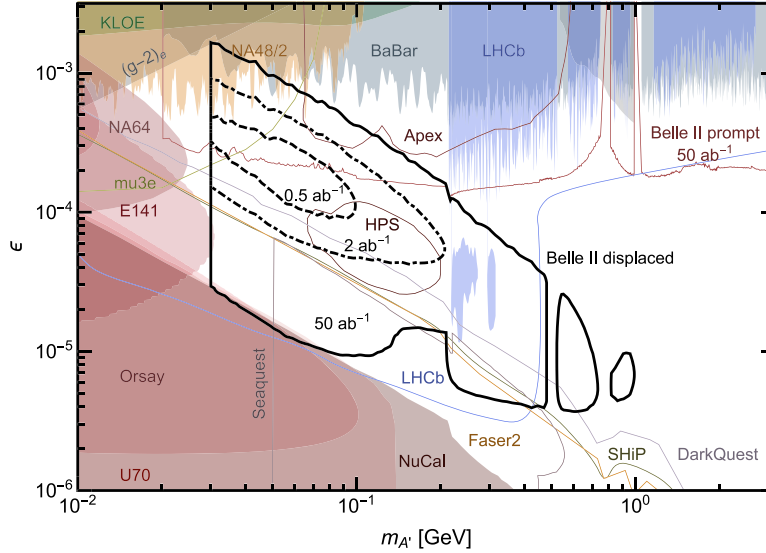


Fig. 4. Overall expected sensitivity of the displaced search at Belle II in the $\epsilon - m_{A'}$ parameter plane compared with other projections assuming an integrated luminosity of 0.5 ab^{-1} (dashed), 2 ab^{-1} (dashed-dotted), and 50 ab^{-1} (solid). Existing limits as well as future projections are taken from [44] except for LHCb [54], HPS [55], SHiP [56] and DarkQuest [57,58]. The Belle II projection for the prompt A' decays is taken from [63].

50 ab^{-1} . As a result, Belle II will become sensitive to this signature only with an integrated luminosity exceeding 2 ab^{-1} .

4.2. Sensitivity for electron final states

The electron final states are experimentally significantly more challenging than the muon final states. Pair conversion events are expected at invariant masses well below 1 MeV. We assume that an invariant mass selection of $m_{ee} \gtrsim 30 \text{ MeV}$ is needed to reject the largest fraction of correctly reconstructed pair conversions due to finite tracking resolution effects. Additional selections on the opening angle θ_{ee} of the daughter electrons are likely needed to increase the tracking efficiency and momentum resolution. In the top panel of Fig. 3 we show the individual sensitivities corresponding to the regions in which $0.2 \text{ cm} < R < 0.9 \text{ cm}$, $17 \text{ cm} < R < 60 \text{ cm}$, and the sensitivity for both regions combined for an angular cut $\theta_{ee} = 0.025$. We observe that a large fraction of the overall sensitivity is due to displacements below 0.9 cm, but also large displacements contribute. As outlined in Sec. 3.3, we expect that additional backgrounds from misreconstructed pair conversions $e^+e^- \rightarrow \gamma\gamma$ cannot be reduced to zero by the selections above. Stronger angular cuts will further reduce backgrounds and we show the sensitivity for different angular cuts θ_{ee} in Fig. 3 (bottom-left). For more optimistic and more pessimistic assumptions on the background levels, we also show the contours for 2.3, 10, 23, and 100 signal events after all selections in Fig. 3 (bottom-right). This corresponds to 90% C.L. sensitivity assuming Poisson statistics for 0, and approximately 50, 300, and 6000 background events in the signal region. As discussed in Sec. 3.3, additional selections may be developed to reduce background from misreconstructed pair conversions which in turn will reduce the signal efficiency. Specifically the sensitivity for 10 events could also be read as an additional reduction of signal efficiency by a factor of 0.23 to reach zero background events.

4.3. Combined sensitivity

In Fig. 4 we show the combined sensitivity taking into all displaced final states, assuming $\theta_{ee} = 0.025$ and 10 events for the electron final state as an optimistic estimate. In addition we show all relevant projections of other future experimental facilities for

comparison. We see that Belle II not only covers a large region of parameter space which is currently still unexplored, but is also uniquely sensitive in particular for dark photon masses close to 1 GeV. As we do not expect any background events in this region, the underlying experimental uncertainties are rather small and our projection therefore correspondingly robust.

5. Discussion

A kinetically mixed dark photon is one of the simplest and most well motivated options to extend the SM of particle physics and has attracted a huge amount of interest over the past couple of years. In this letter we point out that Belle II will be able to probe a significant part of the uncovered parameter space by looking for events with a single high-energy photon and a pair of displaced charged particles. The non-electron final states are experimentally rather straightforward; the electron final states require more detailed experimental studies to reject potentially large backgrounds from misreconstructed pair conversions. We find that while generally a large integrated luminosity will be required to achieve a sufficient sensitivity, Belle II may be able to start probing so far uncovered dark photon parameter space in the near future.

Declaration of competing interest

The authors declare that they have no known competing financial interests or personal relationships that could have appeared to influence the work reported in this paper.

Data availability

Data will be made available on request.

Acknowledgements

We would like to thank Patrick Foldenauer for comments on the draft and for providing the limits from [44] as well as updated data. We thank Christopher Hearty for discussions during early stages of this work, and Isabel Haide for comments on the

manuscript. This work is funded by the Deutsche Forschungsgemeinschaft (DFG) through Germany's Excellence Strategy – EXC 2121 “Quantum Universe” – 390833306 and the Helmholtz (HGF) Young Investigators Grant No. VH-NG-1303. C.G.C. has been supported by the Alexander von Humboldt Foundation during the first stage of this project.

References

- [1] P. Fayet, Extra U(1)'s and new forces, *Nucl. Phys. B* 347 (1990) 743–768.
- [2] B. Patt, F. Wilczek, Higgs-field portal into hidden sectors, arXiv:hep-ph/0605188.
- [3] B. Batell, M. Pospelov, A. Ritz, Exploring portals to a hidden sector through fixed targets, *Phys. Rev. D* 80 (2009) 095024, arXiv:0906.5614.
- [4] B. Holdom, Two U(1)'s and epsilon charge shifts, *Phys. Lett. B* 166 (1986) 196–198.
- [5] M. Ahlers, H. Gies, J. Jaeckel, J. Redondo, A. Ringwald, Light from the hidden sector, *Phys. Rev. D* 76 (2007) 115005, arXiv:0706.2836.
- [6] M. Ahlers, J. Jaeckel, J. Redondo, A. Ringwald, Probing hidden sector photons through the Higgs window, *Phys. Rev. D* 78 (2008) 075005, arXiv:0807.4143.
- [7] B. Batell, M. Pospelov, A. Ritz, Probing a secluded U(1) at B-factories, *Phys. Rev. D* 79 (2009) 115008, arXiv:0903.0363.
- [8] S. Andreas, C. Niebuhr, A. Ringwald, New limits on hidden photons from past electron beam dumps, *Phys. Rev. D* 86 (2012) 095019, arXiv:1209.6083.
- [9] R. Essig, J. Mardon, M. Papucci, T. Volansky, Y.-M. Zhong, Constraining light dark matter with low-energy e^+e^- colliders, *J. High Energy Phys.* 11 (2013) 167, arXiv:1309.5084.
- [10] E. Izaguirre, G. Krnjaic, P. Schuster, N. Toro, New electron beam-dump experiments to search for MeV to few-GeV dark matter, *Phys. Rev. D* 88 (2013) 114015, arXiv:1307.6554.
- [11] D.E. Morrissey, A.P. Spray, New limits on light hidden sectors from fixed-target experiments, *J. High Energy Phys.* 06 (2014) 083, arXiv:1402.4817.
- [12] D. Curtin, R. Essig, S. Gori, J. Shelton, Illuminating dark photons with high-energy colliders, *J. High Energy Phys.* 02 (2015) 157, arXiv:1412.0018.
- [13] M.T. Frandsen, F. Kahlhoefer, A. Preston, S. Sarkar, K. Schmidt-Hoberg, LHC and Tevatron bounds on the dark matter direct detection cross-section for vector mediators, *J. High Energy Phys.* 07 (2012) 123, arXiv:1204.3839.
- [14] M. Fairbairn, J. Heal, F. Kahlhoefer, P. Tunney, Constraints on Z' models from LHC dijet searches and implications for dark matter, *J. High Energy Phys.* 09 (2016) 018, arXiv:1605.07940.
- [15] P. Ilten, Y. Soreq, J. Thaler, M. Williams, W. Xue, Proposed inclusive dark photon search at LHCb, *Phys. Rev. Lett.* 116 (25) (2016) 251803, arXiv:1603.08926.
- [16] M. Battaglieri, et al., US cosmic visions: new ideas in dark matter 2017: community report, in: *U.S. Cosmic Visions: New Ideas in Dark Matter*, 7, 2017, arXiv:1707.04591.
- [17] S. Alekhin, et al., A facility to search for hidden particles at the CERN SPS: the SHiP physics case, *Rep. Prog. Phys.* 79 (12) (2016) 124201, arXiv:1504.04855.
- [18] J. Beacham, et al., Physics beyond colliders at CERN: beyond the standard model working group report, *J. Phys. G* 47 (1) (2020) 010501, arXiv:1901.09966.
- [19] B. Batell, R. Essig, Z. Surujon, Strong constraints on sub-GeV dark sectors from SLAC beam dump E137, *Phys. Rev. Lett.* 113 (17) (2014) 171802, arXiv:1406.2698.
- [20] BaBar, J.P. Lees, et al., Search for invisible decays of a dark photon produced in e^+e^- collisions at BaBar, *Phys. Rev. Lett.* 119 (13) (2017) 131804, arXiv:1702.03327.
- [21] D. Banerjee, et al., Dark matter search in missing energy events with NA64, *Phys. Rev. Lett.* 123 (12) (2019) 121801, arXiv:1906.00176.
- [22] ATLAS, G. Aad, et al., Search for high-mass dilepton resonances in pp collisions at $\sqrt{s} = 8$ TeV with the ATLAS detector, *Phys. Rev. D* 90 (5) (2014) 052005, arXiv:1405.4123.
- [23] LHCb, R. Aaij, et al., Search for $A' \rightarrow \mu^+\mu^-$ decays, *Phys. Rev. Lett.* 124 (4) (2020) 041801, arXiv:1910.06926.
- [24] BaBar, J.P. Lees, et al., Search for a dark photon in e^+e^- collisions at BaBar, *Phys. Rev. Lett.* 113 (20) (2014) 201801, arXiv:1406.2980.
- [25] NA48/2, J.R. Batley, et al., Search for the dark photon in π^0 decays, *Phys. Lett. B* 746 (2015) 178–185, arXiv:1504.00607.
- [26] M.J. Dolan, T. Ferber, C. Hearty, F. Kahlhoefer, K. Schmidt-Hoberg, Revised constraints and Belle II sensitivity for visible and invisible axion-like particles, *J. High Energy Phys.* 12 (2017) 094, arXiv:1709.00009. Erratum: *J. High Energy Phys.* 03 (2021) 190.
- [27] K. Bondarenko, A. Boyarsky, T. Bringmann, M. Hufnagel, K. Schmidt-Hoberg, et al., Direct detection and complementary constraints for sub-GeV dark matter, *J. High Energy Phys.* 03 (2020) 118, arXiv:1909.08632.
- [28] A. Filimonova, R. Schäfer, S. Westhoff, Probing dark sectors with long-lived particles at BELLE II, *Phys. Rev. D* 101 (9) (2020) 095006, arXiv:1911.03490.
- [29] J. Berger, K. Jedamzik, D.G.E. Walker, Cosmological constraints on decoupled dark photons and dark Higgs, *J. Cosmol. Astropart. Phys.* 11 (2016) 032, arXiv:1605.07195.
- [30] S. Biswas, E. Gabrielli, M. Heikinheimo, B. Mele, Higgs-boson production in association with a dark photon in e^+e^- collisions, *J. High Energy Phys.* 06 (2015) 102, arXiv:1503.05836.
- [31] S. Knapen, T. Lin, K.M. Zurek, Light dark matter: models and constraints, *Phys. Rev. D* 96 (11) (2017) 115021, arXiv:1709.07882.
- [32] S. Baek, J. Kim, P. Ko, XENON1T excess in local Z_2 DM models with light dark sector, *Phys. Lett. B* 810 (2020) 135848, arXiv:2006.16876.
- [33] M.J. Dolan, F. Kahlhoefer, C. McCabe, K. Schmidt-Hoberg, A taste of dark matter: flavour constraints on pseudoscalar mediators, *J. High Energy Phys.* 03 (2015) 171, arXiv:1412.5174. Erratum: *J. High Energy Phys.* 07 (2015) 103.
- [34] G. Krnjaic, Probing light thermal dark-matter with a Higgs portal mediator, *Phys. Rev. D* 94 (7) (2016) 073009, arXiv:1512.04119.
- [35] K. Jedamzik, F. Kling, L. Roszkowski, S. Trojanowski, Extending the reach of FASER, MATHUSLA, and SHiP towards smaller lifetimes using secondary particle production, *Phys. Rev. D* 101 (9) (2020) 095020, arXiv:1911.11346.
- [36] E. Izaguirre, G. Krnjaic, B. Shuve, Discovering inelastic thermal-relic dark matter at colliders, *Phys. Rev. D* 93 (6) (2016) 063523, arXiv:1508.03050.
- [37] E. Izaguirre, Y. Kahn, G. Krnjaic, M. Moschella, Testing light dark matter coannihilation with fixed-target experiments, *Phys. Rev. D* 96 (5) (2017) 055007, arXiv:1703.06881.
- [38] A. Berlin, F. Kling, Inelastic dark matter at the LHC lifetime frontier: ATLAS, CMS, LHCb, CODEX-b, FASER, and MATHUSLA, *Phys. Rev. D* 99 (1) (2019) 015021, arXiv:1810.01879.
- [39] M. Duerr, T. Ferber, C. Hearty, F. Kahlhoefer, K. Schmidt-Hoberg, et al., Invisible and displaced dark matter signatures at Belle II, *J. High Energy Phys.* 02 (2020) 039, arXiv:1911.03176.
- [40] M. Duerr, T. Ferber, C. Garcia-Cely, C. Hearty, K. Schmidt-Hoberg, Long-lived dark Higgs and inelastic dark matter at Belle II, *J. High Energy Phys.* 04 (2021) 146, arXiv:2012.08595.
- [41] K.S. Babu, C.F. Kolda, J. March-Russell, Implications of generalized Z - Z-prime mixing, *Phys. Rev. D* 57 (1998) 6788–6792, arXiv:hep-ph/9710441.
- [42] M.T. Frandsen, F. Kahlhoefer, S. Sarkar, K. Schmidt-Hoberg, Direct detection of dark matter in models with a light Z', *J. High Energy Phys.* 09 (2011) 128, arXiv:1107.2118.
- [43] P. Ilten, Y. Soreq, M. Williams, W. Xue, Serendipity in dark photon searches, *J. High Energy Phys.* 06 (2018) 004, arXiv:1801.04847.
- [44] M. Bauer, P. Foldenauer, J. Jaeckel, Hunting all the hidden photons, *J. High Energy Phys.* 07 (2018) 094, arXiv:1803.05466.
- [45] P. Fabbrichesi, E. Gabrielli, G. Lanfranchi, The dark photon, arXiv:2005.01515.
- [46] M. Graham, C. Hearty, M. Williams, Searches for dark photons at accelerators, *Annu. Rev. Nucl. Part. Sci.* 71 (2021) 37–58, arXiv:2104.10280.
- [47] KLOE-2, A. Anastasi, et al., Limit on the production of a new vector boson in $e^+e^- \rightarrow U\gamma$, $U \rightarrow \pi^+\pi^-$ with the KLOE experiment, *Phys. Lett. B* 757 (2016) 356–361, arXiv:1603.06086.
- [48] J.D. Bjorken, R. Essig, P. Schuster, N. Toro, New fixed-target experiments to search for dark gauge forces, *Phys. Rev. D* 80 (2009) 075018, arXiv:0906.0580.
- [49] M. Davier, H. Nguyen Ngoc, An unambiguous search for a light Higgs boson, *Phys. Lett. B* 229 (1989) 150–155.
- [50] J. Blumlein, J. Brunner, New exclusion limits for dark gauge forces from beam-dump data, *Phys. Lett. B* 701 (2011) 155–159, arXiv:1104.2747.
- [51] J. Blümlein, J. Brunner, New exclusion limits on dark gauge forces from proton bremsstrahlung in beam-dump data, *Phys. Lett. B* 731 (2014) 320–326, arXiv:1311.3870.
- [52] NA64, D. Banerjee, et al., Improved limits on a hypothetical X(16.7) boson and a dark photon decaying into e^+e^- pairs, *Phys. Rev. D* 101 (7) (2020), arXiv:1912.11389.
- [53] FASER, A. Ariga, et al., FASER's physics reach for long-lived particles, *Phys. Rev. D* 99 (9) (2019) 095011, arXiv:1811.12522.
- [54] D. Craik, P. Ilten, D. Johnson, M. Williams, LHCb future dark-sector sensitivity projections for Snowmass 2021, in: *2022 Snowmass Summer Study*, 3, 2022, arXiv:2203.07048.
- [55] N. Baltzell, et al., The heavy photon search experiment, arXiv:2203.08324.
- [56] SHiP, C. Ahlida, et al., Sensitivity of the SHiP experiment to dark photons decaying to a pair of charged particles, *Eur. Phys. J. C* 81 (5) (2021) 451, arXiv:2011.05115.
- [57] A. Berlin, S. Gori, P. Schuster, N. Toro, Dark sectors at the Fermilab SeaQuest experiment, *Phys. Rev. D* 98 (3) (2018) 035011, arXiv:1804.00661.
- [58] A. Apyan, et al., DarkQuest: a dark sector upgrade to SpinQuest at the 120 GeV Fermilab main injector, in: *2022 Snowmass Summer Study*, 3, 2022, arXiv:2203.08322.
- [59] M. D'Onofrio, O. Fischer, Z.S. Wang, Searching for dark photons at the LHeC and FCC-he, *Phys. Rev. D* 101 (1) (2020) 015020, arXiv:1909.02312.
- [60] S. Dreyer, et al., Physics reach of a long-lived particle detector at Belle II, arXiv:2105.12962.
- [61] Belle-II, T. Abe, et al., Belle II technical design report, arXiv:1011.0352.
- [62] J. Alwall, R. Frederix, S. Frixione, V. Hirschi, F. Maltoni, et al., The automated computation of tree-level and next-to-leading order differential cross sections,

- and their matching to parton shower simulations, J. High Energy Phys. 07 (2014) 079, arXiv:1405.0301.
- [63] E. Kou, et al., The Belle II physics book, PTEP 2019 (12) (2019) 123C01, arXiv:1808.10567. Erratum: PTEP 2020 (2020) 029201.
- [64] F. Bossi, Dark photon searches using displaced vertices at low energy e^+e^- colliders, Adv. High Energy Phys. 2014 (2014) 891820, arXiv:1310.8181.
- [65] E. Bernreuther, K. Böse, T. Ferber, C. Hearty, F. Kahlhoefer, et al., Forecasting dark showers at Belle II, arXiv:2203.08824.